

Theoretical investigation of potential superconductivity in Sr-doped $La_3Ni_2O_7$ at ambient pressure

Lei Shi(石磊), Ying Luo(罗颖), Wei Wu(吴为), and Yunwei Zhang(张云蔚)

Citation: Chin. Phys. B, 2025, 34 (**7**): 077403. DOI: 10.1088/1674-1056/add1bd
http://cpb.iphy.ac.cn; http://iopscience.iop.org/cpb

What follows is a list of articles you may be interested in

Possible coexistence of superconductivity and topological electronic states in 1T-RhSeTe

Tengdong Zhang(张腾东), Rui Fan(樊睿), Yan Gao(高炎), Yanling Wu(吴艳玲), Xiaodan Xu(徐晓丹), Dao-Xin Yao(姚道新), and Jun Li(李军)
Chin. Phys. B, 2025, 34 (**2**): 027403. DOI: 10.1088/1674-1056/ada432

Surface-sensitive electronic structure of kagome superconductor CsV_3Sb_5

Zhisheng Zhao(赵志生), Jianghao Yao(姚江浩), Rui Xu(徐瑞), Yuzhe Wang(王禹喆), Sen Liao(廖森), Zhengtai Liu(刘正太), Dawei Shen (沈大伟), Shengtao Cui(崔胜涛), Zhe Sun(孙喆), Yilin Wang(王义林), Donglai Feng(封东来), and Juan Jiang(姜娟)
Chin. Phys. B, 2024, 33 (**10**): 107403. DOI: 10.1088/1674-1056/ad7016

Experimental observation of Fermi-level flat band in novel kagome metal $CeNi_5$

Xue-Zhi Chen(陈学智), Le Wang(王乐), Shuai Zhang(张帅), Ren-Jie Zhang(张任杰), Yi-Wei Cheng(程以伟), Yu-Dong Hu(胡裕栋), Cheng-Nuo Meng(孟承诺), Zheng-Tai Liu(刘正太), Bai-Qing Lv(吕佰晴), and Yao-Bo Huang(黄耀波)
Chin. Phys. B, 2024, 33 (**8**): 087402. DOI: 10.1088/1674-1056/ad4019

Electronic structure and effective mass of pristine and Cl-doped $CsPbBr_3$

Zhiyuan Wei(魏志远), Yu-Hao Wei(魏愉昊), Shendong Xu(徐申东), Shuting Peng(彭舒婷), Makoto Hashimoto, Donghui Lu(路东辉), Xu Pan(潘旭), Min-Quan Kuang(匡泯泉), Zhengguo Xiao(肖正国), and Junfeng He(何俊峰)
Chin. Phys. B, 2024, 33 (**5**): 057403. DOI: 10.1088/1674-1056/ad3c31

Superconductivity in kagome metal $ThRu_3Si_2$

Yi Liu(刘艺), Jing Li(厉静), Wu-Zhang Yang(杨武璋), Jia-Yi Lu(卢佳依), Bo-Ya Cao(曹博雅), Hua-Xun Li(李华旬), Wan-Li Chai(柴万力), Si-Qi Wu(武思祺), Bai-Zhuo Li(李佰卓), Yun-Lei Sun(孙云蕾), Wen-He Jiao(焦文鹤), Cao Wang(王操), Xiao-Feng Xu(许晓峰), Zhi Ren(任之), and Guang-Han Cao(曹光旱)
Chin. Phys. B, 2024, 33 (**5**): 057401. DOI: 10.1088/1674-1056/ad1c5e

---

SPECIAL TOPIC — Superconductivity in nickel oxides

Theoretical investigation of potential superconductivity in Sr-doped $La_3Ni_2O_7$ at ambient pressure

Lei Shi(石磊)[1], Ying Luo(罗颖)[1], Wei Wu(吴为)[1,2,†], and Yunwei Zhang(张云蔚)[1,2,‡]

[1] *School of Physics, Sun Yat-sen University, Guangzhou* 510275, *China*

[2] *Guangdong Provincial Key Laboratory of Magnetoelectric Physics and Devices, Sun Yat-sen University, Guangzhou* 510275, *China*

(Received 4 March 2025; revised manuscript received 25 April 2025; accepted manuscript online 29 April 2025)

The recent discovery of pressure-induced superconductivity in $La_3Ni_2O_7$ has established a novel platform for studying unconventional superconductors. However, achieving superconductivity in this system currently requires relatively high pressures. In this study, we propose a chemical pressure strategy via Sr substitution to stabilize high-T_c superconductivity in $La_3Ni_2O_7$ under ambient conditions. Using density functional theory (DFT) calculations, we systematically investigate the structural and electronic properties of Sr-doped $La_{3-x}Sr_xNi_2O_7$ ($x = 0.25, 0.5, 1$) at ambient pressure and identify two dynamically stable phases: $La_{2.5}Sr_{0.5}Ni_2O_7$ and $La_2SrNi_2O_7$. Our calculations reveal that both phases exhibit metallization of the σ-bonding bands dominated by Ni-d_{z^2} orbitals — a key feature associated with high-T_c superconductivity, as reported in the high-pressure phase of $La_3Ni_2O_7$. Further analysis using tight-binding models shows that the key hopping parameters in $La_{2.5}Sr_{0.5}Ni_2O_7$ and $La_2SrNi_2O_7$ closely resemble those of $La_3Ni_2O_7$ under high pressure, indicating that strong super-exchange interactions between interlayer Ni-d_{z^2} orbitals are preserved. These findings suggest that the doped phases may provide a promising platform for exploring superconductivity, which requires further experimental validation.

Keywords: superconducting nickelate, *ab initio* calculations, electronic structure, hole-doped

PACS: 74.20.Pq, 74.72.Gh, 31.15.A–

DOI: 10.1088/1674-1056/add1bd **CSTR:** 32038.14.CPB.add1bd

1. Introduction

Nickelates have long been proposed as candidates for cuprate-like unconventional superconductivity due to the electronic similarities between Ni and Cu. However, experimentally observed superconducting critical temperatures (T_c) in nickelates, such as thin-film $Nd_6Ni_5O_{12}$, $Nd_{1-x}Sr_xNiO_2$ and $Pr_{1-x}Sr_xNiO_2$, remain below the boiling point of liquid (77 K).[1–3] Recently, superconductivity with a T_c of approximately 80 K was discovered in single-crystal $La_3Ni_2O_7$ at high pressure (14.0–43.5 GPa),[4] a finding confirmed by subsequent experimental observations.[5,6] The bilayer Ruddlesden–Popper structure of $La_3Ni_2O_7$ undergoes a pressure-induced phase transition from the orthorhombic *Amam* phase to *Fmmm* phase, coincident with the emergence of superconductivity. It has been demonstrated that the metallization of Ni-d_{z^2} bonding bands in the high-pressure *Fmmm* phase plays an important role in the emergence of the high-T_c state.[4,7–15] However, the requirement of high pressures severely limits the practical application of $La_3Ni_2O_7$.

Beyond high-pressure synthesis, chemical doping is a widely used strategy for tuning lattice and electronic properties of materials, often stabilizing superconductivity at reduced pressures. For example, in LaH_{10}, Y doping increased T_c above 250 K while reducing the required pressure from 200 GPa to 183 GPa.[16–18] In nickelates, Sr doping has been shown to induce superconductivity in infinite-layer $NdNiO_2$ and $PrNiO_2$ films at ambient pressure by modifying Ni-d orbitals occupancy and adjusting the density of states near the Fermi level (E_F).[19–22] These results suggest that chemical doping could provide a promising approach for realizing superconductivity in $La_3Ni_2O_7$ at lower pressures or even ambient conditions.

Recently, Wang *et al.* reported pressure-induced superconductivity with a T_c of 60 K in Pr-doped $La_3Ni_2O_7$.[23,24] Similar to pristine $La_3Ni_2O_7$, the Ni-d_{z^2} orbitals in Pr-doped $La_3Ni_2O_7$ exhibit splitting near the E_F at ambient pressure. Upon applying pressure, the Ni-d_{z^2} bonding bands become metallized, suggesting a superconducting mechanism akin to that of pristine $La_3Ni_2O_7$.[24] However, superconductivity in this system still requires a high pressure exceeding 10 GPa. Several theoretical studies have explored the potential for ambient-pressure superconductivity in $La_3Ni_2O_7$ through full substitution of La with rare-earth elements.[25–27] However, these studies revealed that rare-earth bilayer nickelates are unstable in the superconducting *Fmmm* phase of $La_3Ni_2O_7$ at ambient pressure. Although some stable metallic structures, such as $Tb_3Ni_2O_7$, have been identified, they exhibit signif-

†Corresponding author. E-mail: wuwei69@mail.sysu.edu.cn

‡Corresponding author. E-mail: zhangyunw@mail.sysu.edu.cn

© 2025 Chinese Physical Society and IOP Publishing Ltd. All rights, including for text and data mining, AI training, and similar technologies, are reserved.

icant structural deviations from the *Fmmm* phase, and their superconducting properties have yet to be experimentally verified.

In this work, we systematically investigate the structural and electronic properties of Sr-doped nickelates $La_{3-x}Sr_xNi_2O_7$ ($x = 0.25$, 0.5, 1) at ambient pressure. Among these compositions, we identify two stable phases $La_{2.5}Sr_{0.5}Ni_2O_7$ and $La_2SrNi_2O_7$, which crystalize in the space groups of *Pmma* and *Amam*, respectively. Our density functional theory (DFT) calculations reveal that Sr doping shifts the E_F downward while preserving a band structure similar to that of the superconducting *Fmmm* phase near the E_F. Both doped phases exhibit metallization of Ni-d_{z^2} bonding bands, suggesting a superconducting mechanism akin to that of high-pressure $La_3Ni_2O_7$. Furthermore, our tight-binding model analysis indicates that the key hopping parameters between Ni-3d and O-2p orbitals in $La_{2.5}Sr_{0.5}Ni_2O_7$ and $La_2SrNi_2O_7$ closely resemble those of the high-pressure pristine phase, preserving strong interlayer super-exchange interactions. These results suggest that Sr-doped $La_3Ni_2O_7$ is a promising candidate for achieving superconductivity at ambient pressure.

2. Method

First-principles calculations were performed using DFT as implemented in the Vienna *ab initio* simulation package (VASP).[28,29] The Perdew–Burke–Ernzerhof (PBE)[30] exchange–correlation functional within the generalized gradient approximation (GGA) was employed, with a plane-wave cutoff energy of 600 eV. The projector-augmented wave (PAW) method was used to describe the electron–ion interactions.[31] A $19 \times 19 \times 5$ k-points mesh was used for self-consistent calculations. Atomic positions were fully optimized until the forces on each atom were below 0.001 eV/Å. To account for electron correlation effects, a Hubbard U correction of 4 eV was applied to the Ni 3d electrons using the GGA+U approach.[32,33] Dynamical stability was examined via density functional perturbation theory (DFPT) as implemented in Phononpy.[34] Tight-binding Hamiltonians were constructed using the Wannier90 software package based on maximally localized Wannier functions.[35,36]

3. Results and discussion

The crystal structures of $La_{3-x}Sr_xNi_2O_7$ ($x = 0.25$, 0.5, 1) at ambient pressure are constructed by substituting La with Sr in the *Amam* phase of pristine $La_3Ni_2O_7$. In this phase, two distinct La sites exist, corresponding to the Wyckoff position 4c and 8g, labelled as La1 and La2 in Fig. 1(a). La1 atoms occupy the higher-symmetry 4c sites, positioned between the corner-sharing NiO_6 octahedral layers, while La2 atoms reside at the lower symmetry 8g sites, each coordinated with eight O atoms. For $La_{2.75}Sr_{0.25}Ni_2O_7$, we identify two polymorphs by substituting a single La atom with Sr at different sites within the unit cell. However, both structures exhibit dynamic instability, as indicated by imaginary frequencies in their phonon spectra (Fig. S1 in the supplementary information). For $La_{2.5}Sr_{0.5}Ni_2O_7$ and $La_2SrNi_2O_7$, we examined three types of high-symmetry structures, and select the configuration with the lowest energy for further discussion. Despite the absence of superconductivity observed in recent experiments for Sr-doped $La_3N_2O_7$ with Sr occupying the 8g La sites,[37] our calculations indicate that the lowest-energy structures favor Sr substitution at the 4c position. Detailed structural information and relative energies of all polymorphs for $La_{3-x}Sr_xNi_2O_7$ ($x = 0.5$ and 1) are provided in the supplementary information (Figs. S2 and S3).

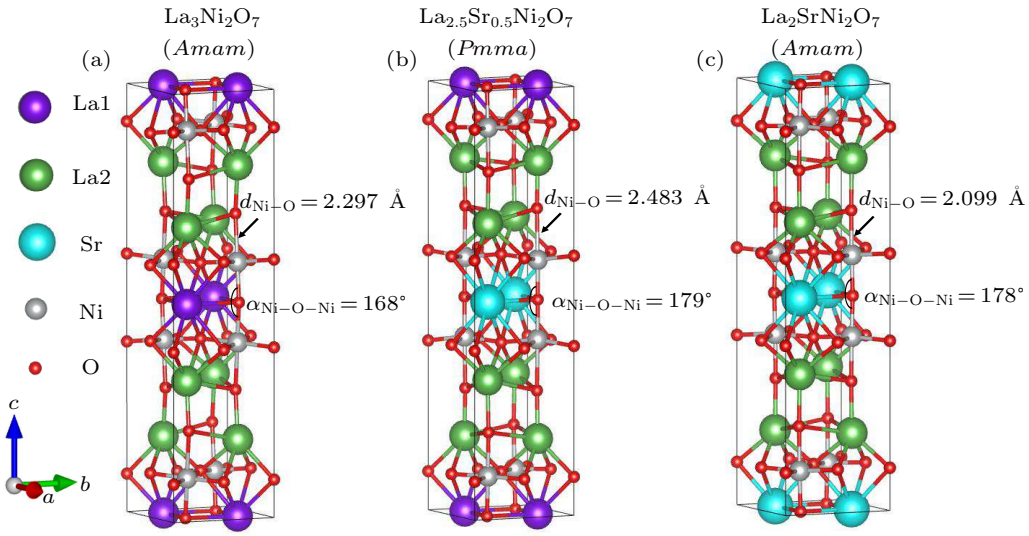


Fig. 1. Crystal structures of $La_{3-x}Sr_xNi_2O_7$ ($x = 0$, 0.5, 1) at ambient pressure: (a) *Amam* phase of $La_3Ni_2O_7$, (b) *Pmma* phase of $La_{2,5}Sr_{0.5}Ni_2O_7$, (c) *Amam* phase of $La_2SrNi_2O_7$. The corresponding Ni–O bond lengths and Ni–O–Ni bond angles are indicated.

$La_{2.5}Sr_{0.5}Ni_2O_7$ adopts a structure with the *Pmma* space group (Fig. 1(b)), while $La_2SrNi_2O_7$ shares the same structural prototype as the *Amam* phase of $La_3Ni_2O_7$ (Fig. 1(c)). Phonon calculations confirm that both structures are dynamically stable (Fig. 2). To further assess the energy stability of $La_{2.5}Sr_{0.5}Ni_2O_7$ and $La_2SrNi_2O_7$, we perform formation energy calculations, comparing the total energies of $La_{2.5}Sr_{0.5}Ni_2O_7 + 0.5La$ and $La_2SrNi_2O_7 + La$ with those of $La_3Ni_2O_7 + 0.5Sr$ and $La_3Ni_2O_7 + Sr$. The calculated energies are -85.12 eV for $La_{2.5}Sr_{0.5}Ni_2O_7 + 0.5La$, -84.74 eV for $La_2SrNi_2O_7 + La$, -86.16 eV for $La_3Ni_2O_7 + 0.5Sr$ and -86.97 eV for $La_3Ni_2O_7 + Sr$. The higher formation energies of $La_{2.5}Sr_{0.5}Ni_2O_7$ and $La_2SrNi_2O_7$ indicate that these compounds are metastable relative to $La_3Ni_2O_7$ and Sr. However, we note that the recently synthesized $La_2PrNi_2O_7$[23,24] is also less energetically favorable than $La_3Ni_2O_7$ and Pr metal. Therefore, despite their metastability, $La_{2.5}Sr_{0.5}Ni_2O_7$ and $La_2SrNi_2O_7$ remain promising candidates for synthesis.

The corresponding structural information is listed in Table 1. In the high-pressure phase of $La_3Ni_2O_7$, the Ni–O (apical oxygen) bond length $d_{(Ni-O)\perp}$ decreases from 2.32 Å to 2.132 Å, while the Ni–O–Ni bond angle increases from 168° to 180°. For $La_{2.5}Sr_{0.5}Ni_2O_7$ at ambient pressure, the $d_{(Ni-O)\perp}$ is 2.483 Å, slightly larger than that of the $La_3Ni_2O_7$ at 29.5 GPa. However, the Ni–O–Ni bond angle α increases significantly to around 179°, indicating that Sr doping induces a chemical pressure effect, which may enhance interlayer coupling. In the case of $La_2SrNi_2O_7$, $d_{(Ni-O)\perp}$ is 2.099 Å, and the Ni–O–Ni bond angle is 178°, both closely resembling those of the high-pressure phase of $La_3Ni_2O_7$ ($d_{(Ni-O)\perp} = 2.132$ Å, $\alpha = 180^{\circ}$). A nonmonotonic evolution of $d_{(Ni-O)\perp}$ exists from $La_{2.5}Sr_{0.5}Ni_2O_7$ to $La_2SrNi_2O_7$, arising from distinct structural changes associated with different doping levels. In $La_{2.5}Sr_{0.5}Ni_2O_7$, only half of the La1 sites are substituted by Sr atoms, resulting in a lower-symmetry *Pmma* structure. In contrast, $La_2SrNi_2O_7$ exhibits full substitution at the La1 sites and adopts a higher-symmetry *Amam* phase, which is isostructural with the ambient-pressure phase of $La_3Ni_2O_7$. The reduced symmetry in $La_{2.5}Sr_{0.5}Ni_2O_7$ creates a more anisotropic chemical environment, which stretches the Ni–O bonds along the out-of-plane direction and leads to a larger $d_{(Ni-O)\perp}$ compared to $La_2SrNi_2O_7$ and pristine $La_3Ni_2O_7$.

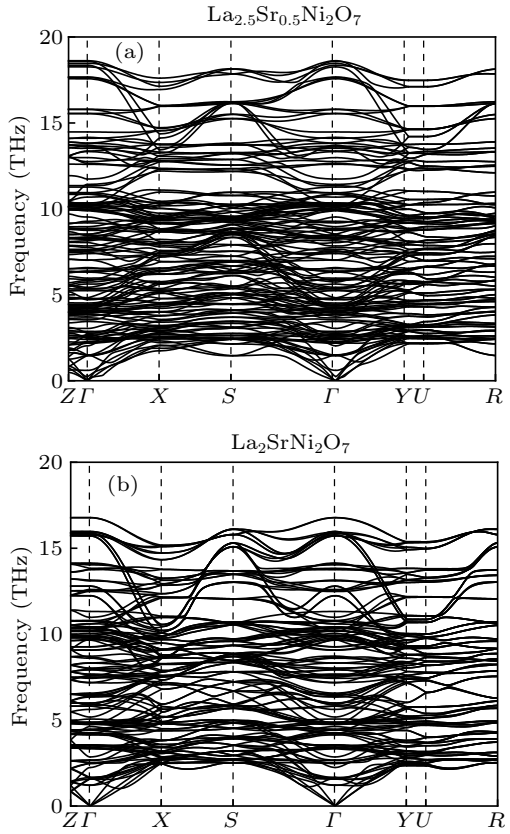


Fig. 2. Phonon dispersion of $La_{2.5}Sr_{0.5}Ni_2O_7$ (a) and $La_2SrNi_2O_7$ (b) at ambient pressure.

Table 1. Structural information of $La_{3-x}Sr_xNi_2O_7$ ($x = 0$, 0.5, 1). The pressure, lattice parameters, in-plane Ni–O bond length ($d_{(Ni-O)\parallel}$), Ni and apical oxygen bond length ($d_{(Ni-O)\perp}$), out-of-plane Ni–O–Ni bond length ($d_{Ni-O-Ni}$) and Ni–O–Ni bond angle (α) are listed.

Compound	a (Å)	b (Å)	c (Å)	$d_{(Ni-O)\parallel}$ (Å)	$d_{(Ni-O)\perp}$ (Å)	$d_{Ni-O-Ni}$ (Å)	α (°)
$La_3Ni_2O_7$ (0 GPa)	5.359	5.413	20.612	1.916	2.320	3.902	168
$La_3Ni_2O_7$ (29.5 GPa)	5.289	5.218	19.734	1.857	2.132	3.795	180
$La_{2.5}Sr_{0.5}Ni_2O_7$ (0 GPa)	5.367	5.359	20.753	1.911	2.483	3.852	179
$La_2SrNi_2O_7$ (0 GPa)	5.443	5.444	20.082	1.926	2.099	3.840	178

We further investigate the electronic properties of these stable phases to explore the potential superconductivity in Sr-doped $La_3Ni_2O_7$. Our band structure calculations for the ambient-pressure *Amam* phase and the superconducting *Fmmm* phase of $La_3Ni_2O_7$ under high pressure (Figs. 3(a) and 3(b)) show excellent agreement with previous theoretical studies.[4] The bands associated with Ni-d_{z^2} bonding states become metallized (shown in blue in Fig. 3(b)) at high pressure, which has been identified as a key indicator of superconductivity.[4,7–15] Similarly, our calculated band structures of $La_{2.5}Sr_{0.5}Ni_2O_7$ and $La_2SrNi_2O_7$ (Figs. 3(c) and 3(d)) at ambient pressure structures also exhibit metallized Ni-d_{z^2} bonding bands. Notably, these band structures near the E_F closely resemble that of the superconducting pristine *Fmmm* phase, where the energy bands of Sr atoms are located at very low energy levels and have a negligible influence on the electronic structures near the E_F.

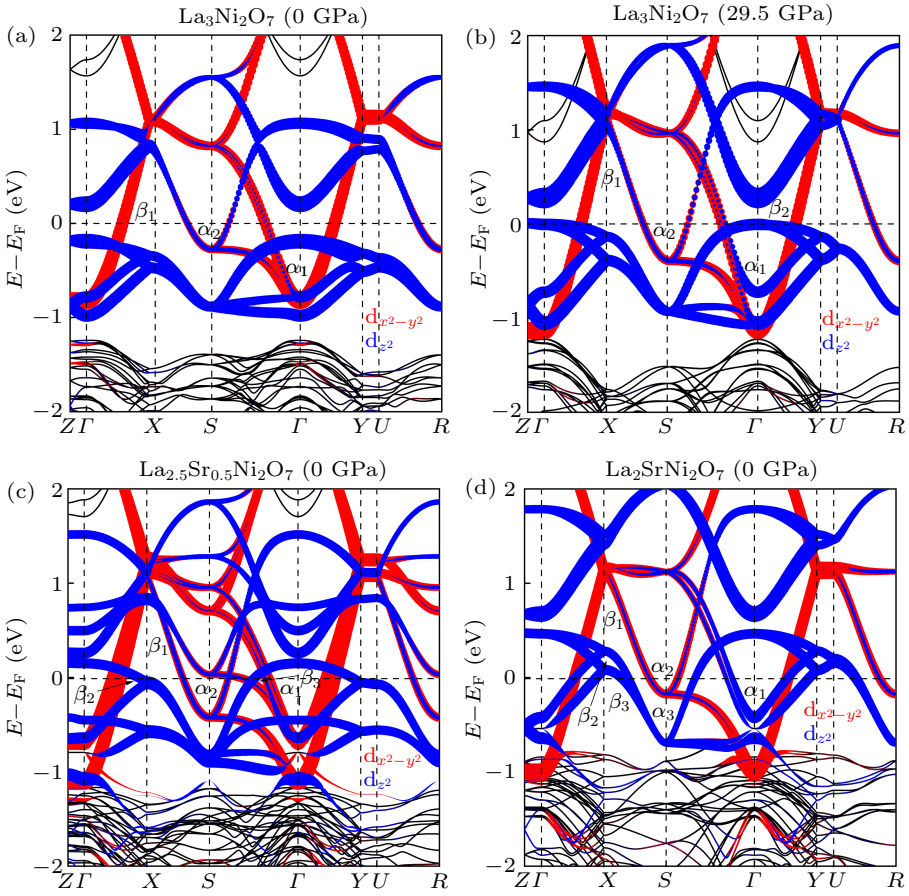


Fig. 3. Band structures of $La_3Ni_2O_7$ at 0 GPa (a) and 29.5 GPa (b), $La_{2.5}Sr_{0.5}Ni_2O_7$ at 0 GPa (c) and $La_2SrNi_2O_7$ at 0 GPa (d). The projections onto Ni-$d_{x^2-y^2}$ and Ni-d_{z^2} orbitals are highlighted in red and blue, respectively. The black dashed lines indicate the Fermi level (E_F) in each panel. α_i and β_i denote electron and hole pockets appeared at the Fermi surface, respectively.

As shown in Figs. 3(c) and 3(d), despite the splitting of degenerate orbitals around S and Z points in $La_{2.5}Sr_{0.5}Ni_2O_7$ due to the reduced symmetry, the key band characteristics associated with the superconductivity in the high-pressure phase of $La_3Ni_2O_7$ are preserved in both $La_{2.5}Sr_{0.5}Ni_2O_7$ and $La_2SrNi_2O_7$. The bonding–antibonding splitting of Ni-d_{z^2} orbitals in $La_{2.5}Sr_{0.5}Ni_2O_7$ and $La_2SrNi_2O_7$ is approximately 1.4 eV, close to the 1.5 eV splitting in the high-pressure pristine phase. This suggests that the interlayer hopping amplitude ($t_\perp$) between Ni-d_{z^2} orbitals remains relatively large in these two Sr-doped structures, maintaining strong interlayer superexchange interactions, which are considered the primary driving force behind superconductivity in the high-pressure phase of $La_3Ni_2O_7$. The electronic interactions between NiO_2 bilayers are not significantly weakened at ambient pressure, indicating that $La_{2.5}Sr_{0.5}Ni_2O_7$ and $La_2SrNi_2O_7$ may exhibit potential superconductivity.

As for the Ni-$d_{x^2-y^2}$ orbitals, the bandwidth in the high-pressure phase of $La_3Ni_2O_7$ is around 4.2 eV (Fig. 3(b)). In comparison, the Ni-$d_{x^2-y^2}$ derived bands in $La_{2.5}Sr_{0.5}Ni_2O_7$ and $La_2SrNi_2O_7$ exhibit similar bandwidths at ambient pressure (Figs. 3(c) and 3(d)), whereas the ambient-pressure phase of $La_3Ni_2O_7$ has a significantly narrower bandwidth of about 3.6 eV (Fig. 3(a)). This suggests that Sr doping effectively induces a chemical pressure effect, replicating the electronic environment of the high-pressure phase.

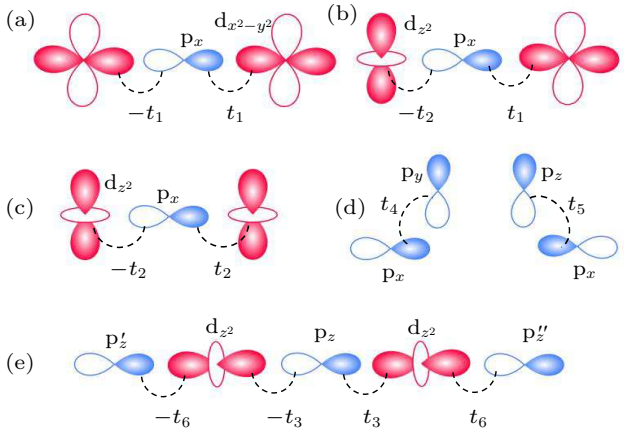


Fig. 4. Six hopping processes between Ni-3d and O-2p orbitals, including Ni-$d_{x^2-y^2}$ and O-p_x (a), Ni-d_{z^2} and O-p_x, O-p_x and Ni-$d_{x^2-y^2}$ (b), Ni-d_{z^2} and O-p_x, (c), O-p_x and O-p_y, O-p_x and O-p_z (d), Ni-d_{z^2} and O-p_z (e). The relevant hopping parameters for $La_{3-x}Sr_xNi_2O_7$ ($x = 0$, 0.5, 1) are listed in Table 2.

Additionally, O-2p orbitals make a significant contribution to the electronic states near the E_F in $La_{2.5}Sr_{0.5}Ni_2O_7$ and $La_2SrNi_2O_7$ (Figs. S4(b) and S4(c) in supplementary information), strongly hybridizing with both Ni-d_{z^2} and Ni-$d_{x^2-y^2}$ orbitals. This hybridization closely resembles that observed

in the high-pressure phase of $La_3Ni_2O_7$ (Fig. S4(a) in supplementary information). Thereby the mobilization of spin-singlet pairs and the global phase coherence are maintained in $La_{2.5}Sr_{0.5}Ni_2O_7$ and $La_2SrNi_2O_7$. Meanwhile, Ni-t_{2g} orbitals in $La_{2.5}Sr_{0.5}Ni_2O_7$ and $La_2SrNi_2O_7$ remain far from the E_F, suggesting they play a minimal role in superconductivity.

Table 2. The hopping parameters between Ni-3d and O-2p of $La_{3-x}Sr_xNi_2O_7$ ($x = 0, 0.5, 1$).

Compound	Pressure (GPa)	t_1	t_2	t_3	t_4	t_5	t_6
$La_3Ni_2O_7$	29.5	−1.56	0.75	−1.63	0.58	0.49	1.37
$La_{2.5}Sr_{0.5}Ni_2O$	0	−1.39	0.64	−1.54	0.59	0.40	0.73
$La_2SrNi_2O_7$	0	−1.39	0.74	−1.56	0.54	0.45	1.25

To further assess the potential for superconductivity in Sr-doped $La_3Ni_2O_7$ at ambient pressure, we construct a tight-binding model for $La_{2.5}Sr_{0.5}Ni_2O_7$ and $La_2SrNi_2O_7$ and compare the relevant hopping parameters with those of $La_3Ni_2O_7$ at high pressure[38,39] (as listed in Table 2). For these two Sr-doped structures, the hopping parameter t_1, which corresponds to the interaction between Ni-$d_{x^2-y^2}$ and O-p_x, is approximately −1.39, slightly smaller than the value in $La_3Ni_2O_7$ at 29.5 GPa ($t_1 = -1.56$). This difference may stem from the larger lattice parameters a and b after Sr doping (Table 1). Another key hopping parameter, t_3, governs the strength of the super-exchange interactions between interlayer Ni-d_{z^2} orbitals. Notably, t_3 remains nearly identical after Sr doping, with values of $t_3 = -1.54$ for $La_{2.5}Sr_{0.5}Ni_2O_7$, $t_3 = -1.56$ for $La_2SrNi_2O_7$, and $t_3 = -1.63$ for $La_3Ni_2O_7$ at 29.5 GPa. This suggests that the effective hopping amplitude $t_\perp$ between interlayer Ni-d_{z^2} orbitals remains relatively large, and that the strong interlayer super-exchange interactions between Ni-d_{z^2} orbitals are maintained in $La_{2.5}Sr_{0.5}Ni_2O_7$ and $La_2SrNi_2O_7$. Furthermore, the other hopping parameters in $La_{2.5}Sr_{0.5}Ni_2O_7$ and $La_2SrNi_2O_7$ closely resemble those in $La_3Ni_2O_7$ at 29.5 GPa. As a result, the energy scales defined by the Fermi energy in the Sr-doped phases align well with those of the superconducting phase at high pressure. This indicates that Sr-doped $La_3Ni_2O_7$ may potentially exhibit superconductivity at ambient pressure.

Sr doping raises the energy of the entire d_{z^2} -derived bonding bands and modifies the Fermi surface of the high-pressure pristine phase via a Lifshitz transition. In $La_{2.5}Sr_{0.5}Ni_2O_7$, the d_{z^2} bonding bands are shifted up by ~ 0.37 eV, resulting in a Fermi surface that is distinct from that of $La_3Ni_2O_7$ under high pressure (Figs. 5(b) and 5(c)). Two new hole pockets (β_2 and β_3) emerge along the Γ–X and Γ–S paths, respectively (Figs. 3(c) and 5(c)). As the doping level increases, the d_{z^2} bonding bands in $La_2SrNi_2O_7$ are further raised to ~ 0.64 eV, leading to the emergence of a new electron pocket (α_3) around the S point and two hole pockets (β_2 and β_3) near the X point (Figs. 3(d) and 5(d)). Importantly, these new electron and hole pockets, primarily composed of Ni-d_{z^2} orbitals, persist at the E_F at ambient pressure and are essential for the emergence of superconductivity. It has been widely discussed that superconductivity in $La_3Ni_2O_7$ follows an s± wave pairing symmetry,[8,14,27,40–42] where spin-singlet pairs form mainly between interlayer Ni-d_{z^2} orbitals within the unit cell, making them localized in the a–b plane. Thus, the deformation of the quasi-2D Fermi surface in $La_{2.5}Sr_{0.5}Ni_2O_7$ and $La_2SrNi_2O_7$, compared to the high-pressure $La_3Ni_2O_7$ (Fig. 5(b)), should have minimal impact on superconductivity.

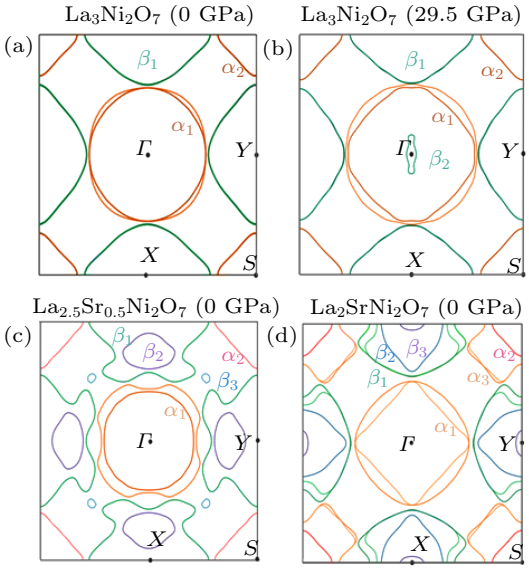


Fig. 5. Fermi surfaces of (a) $La_3Ni_2O_7$ at ambient pressure (b) $La_3Ni_2O_7$ under 29.5 GPa, (c) $La_{2.5}Sr_{0.5}Ni_2O_7$ at ambient pressure, where two new hole pockets β_2 and β_3 appear, and (d) $La_2SrNi_2O_7$ at ambient pressure, where one new electron pocket α_3 and two hole β_2 and β_3 pockets appear. α_i and β_i denote electron and hole pockets, respectively.

4. Conclusion

Our calculations show that Sr doping in $La_3Ni_2O_7$ stabilizes two dynamically stable phases at ambient pressure, $La_{2.5}Sr_{0.5}Ni_2O_7$ and $La_2SrNi_2O_7$, both of which exhibit key features of superconductivity. The preserved electronic structures, including the metallized Ni-d_{z^2} bonding bands and strong interlayer super-exchange interactions, suggest that Sr doping effectively mimics the high-pressure environment necessary for superconductivity. This chemical pressure strategy provides a viable route to achieve potential superconductivity in $La_3Ni_2O_7$ at ambient conditions, eliminating the need for high-pressure synthesis and enabling practical applications.

Acknowledgements

Y.W. Zhang acknowledges funding from the National Key R&D Program of China (Grant No. 2023YFA1610000), the National Natural Science Foundation of China (Grant No. 12304036), the Open Project of Guangdong Provincial Key Laboratory of Magnetoelectric Physics and Devices (Grant No. 2022B1212010008), the Guangdong

Basic and Applied Basic Research Foundation (Grant No. 2023A1515010071), and the Fundamental Research Funds for the Central Universities, Sun Yat-sen University (Grant No. 23xkjc016). W. Wu acknowledges funding from the National Natural Science Foundation of China (Grant Nos. 12494594 and 12274472).

References

[1] Li D F, Lee K, Wang B Y, Osada M, Crossley S, Lee H R, Cui Y, Hikita Y and Hwang H Y 2019 *Nature* **572** 7771
[2] Zeng S W, Tang C S, Yin X M, Li C J, Li M S, Huang Z, Hu J X, Liu W, Omar G J, Jani H, Lim Z S, Han K, Wan D Y, Yang P, Pennycook S J, Wee A T S and Ariando A 2020 *Phys. Rev. Lett.* **125** 147003
[3] Osada M, Wang B Y, Goodge B H, Lee K, Yoon H, Sakuma K, Li D, Miura M, Kourkoutis L F and Hwang H Y 2020 *Nano Lett.* **20** 5735
[4] Sun H L, Huo M W, Hu X W, Li J Y, Liu Z J, Han Y F, Tang L Y, Mao Z Q, Yang P T, Wang B S, Cheng J G, Yao D X, Zhang G M and Wang M 2023 *Nature* **621** 7979
[5] Hou J, Yang P T, Liu Z Y, Li J Y, Shan P F, Ma L, Wang, Wang N N, Guo H Z and Sun J P 2023 *Chin. Phys. Lett.* **40** 117302
[6] Zhang Y N, Su D J, Huang Y N, Shan Z Y, Sun H L, Huo M W, Ye K X, Zhang J W, Yang Z H, Xu Y K, Su Y and Li R, Smidman M, Wang M, Jiao L and Yuan H Q 2024 *Nat. Phys.* **20** 1269
[7] Gu Y H, Le C C, Yang Z S, Wu X X and Hu J P 2025 *Phys. Rev. B* **111** 174506
[8] Yang Q G, Wang D and Wang Q H 2023 *Phys. Rev. B* **108** L140505
[9] Lechermann F, Gondolf J, Bötzel S and Eremin I M 2023 *Phys. Rev. B* **108** L201121
[10] Shen Y, Qin M and Zhang G M 2023 *Chin. Phys. Lett.* **40** 127401
[11] Sakakibara H, Kitamine N, Ochi M and Kuroki K 2024 *Phys. Rev. Lett.* **132** 106002
[12] Liao Z G, Chen L, Duan G J, Wang Y M, Liu C L, Yu R and Si Q M 2023 *Phys. Rev. B* **108** 214522
[13] Yang Y F, Zhang G M and Zhang F C 2023 *Phys. Rev. B* **108** L201108
[14] Yang J G, Sun H L, Hu X W, Xie Y Y, Miao T M, Luo H L, Chen H, Liang B, Zhu W P, Qu Z X, Chen C Q, Huo M W, Huang Y B, Zhang S J, Zhang F F, Yang F, Wang Z M, Peng Q J, Mao H Q, Liu G D, Xu Z Y, Qian T, Yao D X, Wang M, Zhao L and Zhou X J 2024 *Nat. Commun.* **15** 4373
[15] Chen Y, Tian Y H, Wang J M, He R Q and Lu Z Y 2024 *Phys. Rev. B* **110** 235119
[16] Somayazulu M, Ahart M, Mishra A, Geballe Z, Baldini M, Meng Y, Struzhkin V and Hemley R 2019 *Phys. Rev. Lett.* **122** 027001
[17] Semenok D V, Troyan I A, Ivanova A G, Kvashnin A G, Kruglov I A, Hanfland M, Sadakov A V, Sobolevskiy O A, Pervakov K S, Lyubutin I S, Glazyrin K V, Giordano N, Karimov D N, Vasiliev A L, Akashi R, Pudalov V M and Oganov A R 2021 *Materials Today* **48** 18
[18] Song H, Duan D F, Cui T and Kresin V Z 2020 *Phys. Rev. B* **102** 014510
[19] Lee K, Wang B Y, Osada M, Goodge B H, Wang T C, Lee Y, Harvey S, Kim W J, Yu Y, Murthy C, Raghu S, Kourkoutis L F and Hwang H Y 2023 *Nature* **619** 7969
[20] Leonov I, Skornyakov S L and Savrasov S Y 2020 *Phys. Rev. B* **101** 241108
[21] Liu Z, Xu C, Cao C, Zhu W, Wang Z F and Yang J 2021 *Phys. Rev. B* **103** 045103
[22] Wang N N, Yang M W, Yang Z, Chen K Y, Zhang H, Zhang Q H, Zhu Z H, Uwatoko Y, Gu L, Dong X L, Sun J P, Jin K J and Cheng J G 2022 *Nat. Commun.* **13** 4367
[23] Wang N N, Wang G, Shen X L, Hou J, Luo J, Ma X P, Yang H X, Shi L F, Dou J, Feng J, Yang J, Shi Y Q, Ren Z A, Ma H M, Yang P T, Liu Z Y, Liu Y, Zhang H, Dong X L, Wang Y X, Jiang K, Hu J P, Nagasaki S, Kitagawa K, Calder S, Yan J Q, Sun J P, Wang B S, Zhou R, Uwatoko Y and Cheng J G 2024 *Nature* **634** 579
[24] Wang G, Wang N N, Wang Y X, Shi L F, Shen X L, Hou J, Ma H M, Yang P T, Liu Z Y, Zhang H, Dong X L, Sun J P, Wang B S, Jiang K, Hu J P, Uwatoko Y and Cheng J G 2023 arXiv 2311 08212
[25] Geisler B, Hamlin J J, Stewart G R, Hennig R G and Hirschfeld P 2024 *npj Quantum Materials* **9** 38
[26] Pan Z, Lu C, Yang F and Wu C 2024 *Chin. Phys. Lett.* **41** 087401
[27] Zhang Y, Lin L F, Moreo A, Maier T A and Dagotto E 2023 *Phys. Rev. B* **108** 165141
[28] Kresse G and Furthmüller J 1996 *Phys. Rev. B* **54** 11169
[29] Kresse G and Furthmüller J 1996 *Computational Materials Science* **6** 15
[30] Perdew J P, Burke K and Ernzerhof M 1996 *Phys. Rev. Lett.* **77** 3865
[31] Löchl P E 1994 *Phys. Rev. B* **50** 17953
[32] Liechtenstein A I, Anisimov V I and Zaanen J 1995 *Phys. Rev. B* **52** R5467
[33] Dudarev S L, Botton G A, Savrasov S Y, Humphreys C J and Sutton A P 1998 *Phys. Rev. B* **57** 1505
[34] Togo A, Chaput L, Tadano T and Tanaka I 2023 *J. Phys.: Condens. Matter* **35** 353001
[35] Mostofi A A, Yates J R, Pizzi G, Lee Y S, Souza I, Vanderbilt D and Marzari N 2014 *Computer Physics Communications* **185** 2309
[36] Mostofi A A, Yates J R, Lee Y S, Souza I, Vanderbilt D and Marzari N 2008 *Computer Physics Communications* **178** 685
[37] Xu M Y, Huyan S, Wang H Z, Bud'ko S L, Chen X L, Ke X L, Mitchell J F, Canfield P C, Li J and Xie W W 2024 *Advanced Electronic Materials* **10** 2400078
[38] Luo Z H, Hu X W, Wang M, Wú W and Yao D X 2023 *Phys. Rev. Lett.* **131** 126001
[39] Wú W, Luo Z H, Yao D X and Wang M 2024 *Sci. China Phys., Mech. & Astron.* **67** 117402
[40] Liu Y B, Mei J W, Ye F, Chen W Q and Yang F 2023 *Phys. Rev. Lett.* **131** 236002
[41] Zhang Y, Lin L F, Moreo A, Maier T A and Dagotto E 2024 *Nat. Commun.* **15** 2470
[42] Tian Y H, Chen Y, Wang J M, He R Q and Lu Z Y 2024 *Phys. Rev. B* **109** 165154